Inorganic Chemistry

Article

Studies of Structural Effects on the Half-Wave Potentials of Mononuclear and Dinuclear Nickel(II) Diphosphine/Dithiolate Complexes

Kendra Redin, Aaron D. Wilson, Rachel Newell, M. Rakowski DuBois, and Daniel L. DuBois*

Contribution from the Department of Chemistry and Biochemistry, University of Colorado, Boulder, Colorado 80309, and the Division of Chemical Sciences, Pacific Northwest National Laboratory, Richland, Washington 99352

Two series of mononuclear Ni(II) complexes of the formula (PNP)Ni(dithiolate) where PNP = $R_2PCH_2N(CH_3)CH_2$-PR_2, R = Et and Ph, have been synthesized containing dithiolate ligands that vary from five- to seven-membered chelate rings. Two series of dinuclear Ni(II) complexes of the formula $\{[(diphosphine)Ni]_2(dithiolate)\}(X)_2$ (X = BF_4 or PF_6) have been synthesized in which the chelate ring size of the dithiolate and diphosphine ligands have been systematically varied. The structures of the alkylated mononuclear complex, $[(PNP^{Et})Ni(SC_2H_4SMe)]OTf$, and the dinuclear complex, $[(dppeNi)_2(SC_3H_6S)](BF_4)_2$, have been determined by X-ray diffraction studies. The complexes have been studied by cyclic voltammetry to determine how the half-wave potentials of the Ni(II/I) couples vary with chelate ring size of the ligands. For the mononuclear complexes, this potential becomes more positive as the natural bite angle of the dithiolate ligand increases. However, the potentials of the Ni(II/I) couples of the dinuclear complexes do not show a dependence on the chelate ring size of the ligands. Other aspects of the reduction chemistry of these complexes have been explored.

Introduction

Previous studies in our laboratories on simple synthetic nickel bis(diphosphine) complexes have focused on a fundamental understanding of the factors controlling the half-wave potentials of these complexes and the thermodynamic properties of the metal–hydrogen bonds in their corresponding hydride complexes.[1–5] A significant finding in these studies is that the potential of the Ni(II/I) couple becomes more positive as the chelate bite size or natural bite angle of the ligand increases,[1] and this systematic variation can therefore be used to control the potential of this couple. Similarly, the hydride-acceptor abilities of the [Ni(diphosphine)$_2$]$^{2+}$ complexes, as defined by the free energy of the reaction $NiL_n^{2+} + H^- \rightarrow HNiL_n^+$ in solution, have been

shown to exhibit a linear correlation with the potentials of the Ni(II/I) couples.[2] Consequently, as the natural bite angles of the ligands increase, the hydride acceptor abilities of these complexes increase, and large bite angles favor the heterolytic activation of hydrogen. These systematic changes are related to a tetrahedral distortion of the square planar nickel(II) complexes as ligand bite angles increase.

We were interested in determining whether similar relationships between ligand bite angles and half-wave potentials hold for Ni(II) complexes with other types of chelating ligands. For example, the replacement of one diphosphine ligand with a dithiolate results in significant changes in both the steric and electronic features of the nickel complexes. Steric interactions of the phosphorus substituents will be minimized, while the π interactions with the metal ion may be significantly increased with thiolate coordination.[6] As a result, it is not clear whether the relationships observed between chelate bite size and half-wave potentials will hold for square planar Ni complexes that include dithiolate ligands. In this paper we report a new series of Ni(PNP)-(dithiolate) complexes and systematic studies on how the potentials of the Ni(II/I) couples vary with chelate bite angles

---

* To whom correspondence should be addressed. E-mail: daniel.dubois@pnl.gov.

(1) Berning, D.; Noll, B.; DuBois, D. *J. Am. Chem. Soc.* **1999**, *121*, 11432−11447.

(2) Berning, D.; Miedaner, A.; Curtis, C. J. Noll, B. C.; Rakowski DuBois, M.; DuBois, D. L. *Organometallics* **2001**, *20*, 1832−1839.

(3) Curtis, C.; Miedaner, A.; Raebiger, J.; DuBois, D. L. *Organometallics* **2004**, *23*, 511−516.

(4) Curtis, C.; Miedaner, A.; Ellis, W. W.; DuBois, D. L. *J. Am. Chem. Soc.* **2002**, *124*, 1918−1925.

(5) Miedaner, A.; Haltiwanger, R. C.; DuBois, D. L. *Inorg. Chem.* **1991**, *30*, 417.

(6) Ashby, M. T.; Enemark, J. H.; Lichtenberger, D. L. *Inorg. Chem.* **1988**, *27*, 191−197.

of the sulfur donor ligands. In addition, new dinuclear nickel complexes with bridging dithiolate ligands of the formulas [(diphosphine)Ni]$_2$(μ-dithiolate)$^{2+}$ have also been synthesized. The chelate bite sizes of both the diphosphine and dithiolate ligands in this series have been systematically varied with the objective of determining if ligand bite angles can be used to control electrochemical and chemical reduction processes.

This fundamental study of nickel complexes with thiolate donors is prompted in part by the composition of important nickel enzymes. For example, a major class of the hydrogenase enzymes contains a dinuclear Ni−Fe active site in which the nickel ion is coordinated by terminal and bridging cysteine ligands.[7] Both the A-cluster and C-cluster active sites in bifunctional CO dehydrogenase/acetyl CoA synthase enzymes contain dinuclear or cluster complexes in which nickel is coordinated by cysteinyl sulfur donors.[8,9] In the enzymes, the coordination geometry about the nickel atom in the active sites appears to be controlled by the steric constraints imposed by the protein matrix of the enzymes. Distortions from planar or tetrahedral nickel geometries may influence the reduction potentials and reactivities of the active sites. However, a clear relationship between structural distortions and redox potentials has not been established for nickel thiolate structures.

Results and Discussion

Syntheses of Mononuclear Ni Diphosphine/Dithiolate Complexes. Many nickel complexes with mixed phosphine/thiolate ligation have been synthesized previously.[10] In this work, a series of related (PNP^{Et})Ni(II) complexes (where PNP^{Et} = Et$_2$PCH$_2$N(CH$_3$)CH$_2$PEt$_2$) have been synthesized that incorporate anionic sulfur chelates. These include Ni-

(PNP^{Et})(S$_2$CNEt$_2$)]BF$_4$ (**1a**), Ni(PNP^{Et})(SC$_2$H$_4$S) (**2a**), Ni-(PNP^{Et})(SC$_3$H$_6$S) (**3a**), and Ni(PNP^{Et})(SCH$_2$(C$_6$H$_4$)CH$_2$S) (**4a**) in which the size of the metal−sulfur chelate ring varies from four to seven atoms. A second analogous series of complexes of the formula Ni(diphosphine)(dithiolate) (**1b**−**4b**) was prepared using the phenyl-substituted PNP ligand, Ph$_2$PCH$_2$NMeCH$_2$PPh$_2$, PNP^{Ph}. The syntheses of each of the dithiolate complexes followed a similar route in which [Ni-(CH$_3$CN)$_6$](BF$_4$)$_2$ was reacted with an equivalent of PNP^{Et} or PNP^{Ph} and an equivalent of the dithiol in the presence of NEt$_3$, e.g. eq 1 for **2**.

$$[Ni(CH_3CN)_6]^{2+} + PNP + HSC_2H_4SH + 2NEt_3 \rightleftharpoons$$
$$Ni(PNP)(SC_2H_4S) + 2[HNEt_3]^+ \quad (1)$$

Complexes were isolated as orange or red crystalline solids and characterized by spectroscopic techniques, including ^{1}H and ^{31}P NMR, and electrospray mass spectroscopy. Each of the complexes shows a singlet in the ^{31}P NMR spectrum between 9 and 15 ppm, and in most cases m/z values that correspond to the parent ions are observed in the mass spectra.

Attempts were made to synthesize related nickel complexes with thioether ligands for comparative purposes. A thiolate/thioether complex, [(PNP^{Et})Ni(MeSC$_2$H$_4$S)]OTf (**5**), was synthesized by the addition of methyl triflate to the corresponding dithiolate complex. In this reaction, the methylation of the nitrogen base is competitive and ∼20% of the N-methylated cation (**6**) is observed in the NMR spectrum, eq 2. The latter cation was found to react with
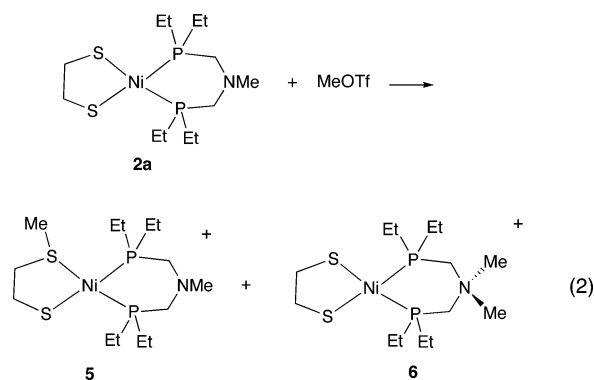

tetramethylguanidine to reform the neutral starting material, which could then be readily separated from the desired cationic thiolate/thioether complex (**5**) by toluene extraction. The ^{31}P NMR spectrum of the cationic thioether complex, isolated by this route, showed a single AB pattern at 4.7 and 17.2 ppm.

An X-ray diffraction study was carried out on a single crystal of **5**. A perspective drawing of the cation structure is shown in Figure 1, and selected bond distances and angles are given in Table 1.

The structural parameters of the PNP^{Et} ligand, which adopts a chair conformation, are similar to those observed previously for [Ni(PN^{Bu}P)$_2$]$^{2+}$ and [Ni(PN^{Me}P)(dmpm)]$^{2+}$ (where PN^{Bu}P = Et$_2$PCH$_2$N(Bu)CH$_2$PEt$_2$, PN^{Me}P = Et$_2$-PCH$_2$N(Me)CH$_2$PEt$_2$, and dmpm = Me$_2$PCH$_2$PMe$_2$).[11] The structure of **5** shows relatively little distortion from a square planar geometry. The bite angle of the diphosphine ligand

(7) (a) Higuchi, Y.; Yagi, T.; Yasuoka, N. *Structure* **1997**, *167*, 1671−1680. (b) Ogata, H.; Mizoguchi, Y.; Mizuno, N.; Miki, K.; Adachi, S.; Yasuoka, N.; Yagi, T.; Yamauchi, O. Hirota, S.; Higuchi, Y. *J. Am. Chem. Soc.* **2002**, *124*, 11628−11635. (c) Volbeda, A.; Garcin, E.; Piras, C.; de Lacey, A.; Fernandez, V. M.; Hatchikian, E. C.; Frey, M.; Fontecilla-Camps, J. *J. Am. Chem. Soc.* **1996**, *118*, 12989−12996.

(8) (a) Doukov, T. L.; Iverson, T. M.; Seravalli, J.; Ragsdale, S. W.; Drennan, C. L. *Science* **2002**, *298*, 567. (b) Darnault, C.; Volbeda, A.; Kim, E. J.; Legrand, P.; Vernede, X.; Lindahl, P. A. ; Fontecilla-Camps, J. C. *Nat. Struct. Biol.* **2003**, *10*, 271−279.

(9) (a) Dobbek, H.; Svetlitchnyi, V.; Gremer, L.; Huber, R.; Meyer, O. *Science,* **2001**, *293*, 1281−1285. (b) Dobbek, H.; Svetlitchnyi, V.; Liss, J.; Meyer, O. *J. Am. Chem. Soc.* **2004**, *126*, 5382−5387. (c) Doukov, T. I.; Iverson, T. M.; Seravalli, J.; Ragsdale, S. W.; Drennan, C. L. *Science* **2002**, *298*, 567−572. (d) Volbeda, A.; Fontecilla-Camps, J. C. *Dalton Trans.* **2005**, 3443−3450.

(10) Autissier, V.; Clegg, W.; Harrington, R. W.; Henderson, R. A. *Inorg. Chem.* **2004**, *43*, 3098. (b) Autissier, V.; Zarza, P. M.; Petrou, A.; Henderson, R. A.; Harrington, R. W.; Clegg, W. C.; *Inorg. Chem.* **2004**, *43*, 3106. (c) Lee, C. M.; Chen, C. H.; Ke, S. C.; Lee, G. H.; Liaw, W. F. *J. Am. Chem. Soc.* **2004**, *126*, 8406. (d) Martins, M. A. C.; Silva, R. M.; Huffman, J. C. *Polyhedron* **2002**, *21*, 421. (e) Tenorio, M. J.; Puerta, M. C.; Valerga, P. *J. Chem. Soc., Dalton Trans.* **1996**, 1935. (f) Hsiao, Y. M.; Chojnacki, S. S.; Hinton, P.; Reibenspies, J. H.; Darensbourg, M. Y. *Organometallics* **1993**, *12*, 870. (g) Bowmaker, G. A.; Boyd, P. D. W.; Campbell, G. K. *Inorg. Chem.* **1982**, *21*, 2403. (h) Rauchfuss, T. B.; Roundhill, D. M. *J. Am. Chem. Soc.* **1975**, *97*, 3386. (i) Darkwa, J. *Inorg. Chim Acta* **1997**, *257*, 137. (j) Pfeiffer, E.; Pasquier, M. L.; Marty, W. *Helv. Chim. Acta* **1984**, *67*, 654. (k) Schmidt, M.; Hoffmann, G. G. *J. Organomet. Chem.* **1977**, *124*, C5.

(11) Curtis, C. J.; Miedaner, A.; Ciancanelli, R.; Ellis, W. W.; Noll, B. C.; DuBois, M. R.; DuBois, D. L. *Inorg. Chem.* **2003**, *42*, 216.
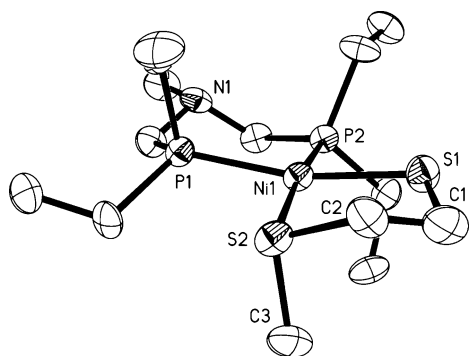
Figure 1. Drawing of the cation of [Ni(PNP)(SC₂H₂SCH₃)]OTf, **5**, showing the atom numbering scheme. Thermal ellipsoids are shown at 50% probability level.

Table 1. Selected Bond Distances (Å), Bond Angles (deg), and Dihedral Angles (deg) for [Ni(PNP^{Et})(SC₂H₄SCH₃)](OTf), **5**

Bond Distances			
Ni(1)−P(1)	2.183(2)	S(1)−C(1)	1.845(8)
Ni(1)−P(2)	2.179(2)	S(2)−C(2)	1.815(8)
Ni(1)−S(1)	2.188(2)	S(2)−C(3)	1.801(8)
Ni(1)−S(2)	2.208(2)	C(1)−C(2)	1.552(1)
Ni(1)···N(1)	3.781(10)		

Bond Angles			
P(1)−Ni(1)−P(2)	91.93(8)	Ni(1)−S(1)−C(1)	106.55(33)
S(1)−Ni(1)−S(2)	90.45(8)	Ni(1)−S(2)−C(2)	103.98(28)
P(1)−Ni(1)−S(2)	91.66(8)	Ni(1)−S(2)−C(3)	101.38(31)
P(2)−Ni(1)−S(1)	87.77(8)	C(2)−S(2)−C(3)	102.82(43)
P(1)−Ni(1)−P(2)···S(1)−Ni(1)−S(2)			15.58(9)

is slightly larger than that of the thiolate/thioether ligand, but both bite angles are near 90°. The dihedral angle between the two planes defined by the P−Ni−P and S−Ni−S atoms is 15.6°. In the structure of [Ni(PN^{Bu}P)₂]²⁺ a significantly larger dihedral angle between the two chelating ligands was observed (34.1°) as a result of steric interactions between ethyl substituents on all four phosphorus donors.

Synthesis of Dinuclear Complexes [(μ-dithiolate)Ni₂-(diphosphine)₂]²⁺. Few examples of the bis(thiolate) bridged dinuclear nickel structure with phosphine ligands have been reported previously.[10i,12] The neutral bis(sulfido) bridged dimer [(dippe)Ni(μ-S)]₂ has been synthesized and structurally characterized, and double alkylation with methyl triflate formed the bis(thiolate) derivative, [(dippe)Ni(μ-SMe)]₂-(OTf)₂,[12] where dippe = bis(diisopropylphosphino)ethane]. However, electrochemical studies of this derivative were not pursued. It is interesting that attempts to react the neutral sulfido-bridged dimer with 1,3-dichloropropane to form a dithiolate-bridged derivative were reported to be unsuccessful, resulting instead in the formation of the mononuclear complexes (dippe)Ni(S₂C₃H₆) and (dippe)NiCl₂.[12b]

In this work, a series of dithiolate-bridged dimers have been successfully synthesized by reaction of (dppe)Ni-(dithiolate)[10g,h,k] (where dppe = 1,2-bis(diphenylphosphino-ethane) with [Ni(CH₃CN)₆](BF₄)₂ in the presence of 1 equiv of dppe, carried out at room temperature in acetonitrile solution (e.g., eq 3 for complex **8**). The resulting red products are formulated as [(μ-dithiolate)Ni₂(dppe)₂](BF₄)₂ (**7−9**)

(12) (a) Vicic, D. A.; Jones, W. D. *J. Am. Chem. Soc.* **1999**, *121*, 7606. (b) Oster, S. S.; Lachicotte, R. J.; Jones, W. D. *Inorg. Chim. Acta* **2002**, *330*, 118.

(3)
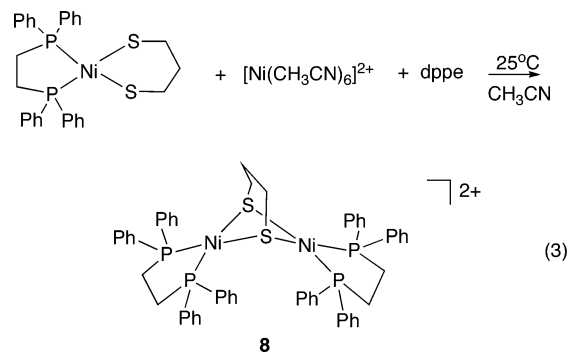
where the backbone of the dithiolate ligand has been varied from two to four carbons (dithiolate = 1,2-SC₂H₄S, 1,3-SC₃H₆S, o-SCH₂C₆H₄CH₂S), respectively.

A slightly different procedure was used to prepare the series of related propanedithiolate-bridged nickel dimers with a variation in chelating diphosphine ligands. The reaction of 2 equiv of Ni(diphosphine)Cl₂[13,14] with 1,3-propanedithiol and excess triethylamine in chloroform led to the formation of [(μ-SC₃H₆S)Ni₂(diphosphine)₂]²⁺ complexes (**10−12**),-which were isolated as the PF₆ salts [diphosphine = dppp (1,3-bis(diphenylphosphino)propane), **10**; dmpp (1,3-(dimethylphosphino)propane), **11**; and dppx (α,α′-bis(diphe-


(4)

diphosphine = dppp, dmpp, dppx
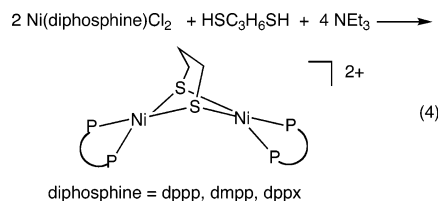
nylphosphino)o-xylene), **12**), eq 4. Together with the dppe complex **8**, discussed above, this series of complexes provides a comparison of diphosphine ligands with five-, six-, and seven-membered chelate rings.

Characterization of all of the new compounds by ¹H and ³¹P NMR spectroscopy, mass spectroscopy, and elemental analyses support their formulation. For example, the ESI mass spectrum of [(μ-SC₂H₄S)Ni₂(dppe)₂][BF₄]₂ showed a strong pattern centered at m/z = 1091 that corresponds to the loss of one BF₄ ion from the dinuclear complex, and a single resonance in the ³¹P NMR spectrum was observed at 59.8 ppm in CDCl₃. In the room-temperature ³¹P NMR spectrum of the product with the xylenedithiolate bridge, **9**, two phosphorus singlets were observed, suggesting that the rate of inversion for the backbone of the dithiolate ligand is slow on the NMR time scale. Variable-temperature NMR studies indicated that coalescence of the two peaks occurred at 38 °C, and the coalescence temperature was used to estimate a ΔG$^{\pm}$ of 19 kcal/mol for this inversion process.[15] In the spectra of [(μ-SC₃H₆S)Ni₂((dppe)₂]²⁺, we were unable to detect evidence for inequivalent diphosphine ligands that

(13) Van Hecke, G. R.; Horrocks, W. D. *Inorg. Chem.* **1966**, *5*, 1968. (b) Booth, G.; Chatt, L. *J. Chem. Soc.* **1965**, 3238.
(14) (a) Brown, M. D.; Levason, W.; Reid, G.; Watts, R. *Polyhedron* **2005**, *24*, 75. (b) Camalli, M.; Caruso, F.; Chaloupka, S.; Leber, E. M.; Rimml, H.; Venanzi, L. M. *Helv. Chim. Acta* **1990**, *73*, 2263.
(15) Williams, D. H.; Fleming, I. *Spectroscopic Methods in Organic Chemistry*, 5th ed.; McGraw-Hill: London, 1995; pp 102−105.
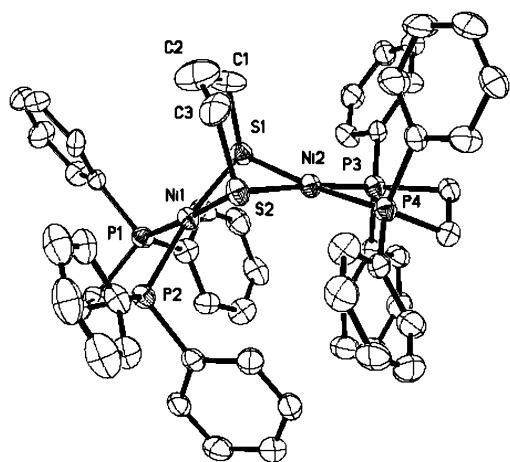
Figure 2. Perspective drawing of $[(\mu\text{-}SC_3H_6S)Ni_2(dppe)_2]^{2+}$, **8**. Thermal ellipsoids are shown at the 50% probability level.

Table 2. Selected Bond Distances and Angles for $[(\mu\text{-}SC_3H_6S)Ni_2(dppe)_2](BF_4)_2$, **8**

distances, Å		angles, deg	
Ni(1)−P(1)	2.175 (2)	P(1)−Ni(1)−P(2)	86.44(7)
Ni(1)−P(2)	2.164(2)	P(1)−Ni(1)−S(1)	91.11(7)
Ni(1)−S(1)	2.221 (2)	P(2)−Ni(1)−S(1)	169.89(8)
Ni(1)−S(2)	2.217 (2)	P (1)-Ni(1)−S(2)	176.86(8)
Ni(2)−P(3)	2.182 (2)	P(2)−Ni(1)−S(2)	95.85(7)
Ni(2)−P(4)	2.181(2)	Ni(1)−S(1)−Ni(2)	80.37(6)
Ni(2)−S(1)	2.228(2)	Ni(1)−S(2)−Ni(2)	80.57(6)

would result from a rigid orientation of the propanedithiolate bridge. A single ^{31}P resonance was observed near 60 ppm in the low-temperature ^{31}P NMR spectra at temperatures down to −80 °C in CD_2Cl_2. These ligand differences are similar to those reported for $[(CO)_3Fe]_2(\mu\text{-dithiolate})$ complexes in which inversion of the ligand backbone of the xylenedithiolate complex was not observed by NMR spectroscopy while fluxional behavior was seen for the analogous propanedithiolate complex.[16]

X-ray Diffraction Study of $[(\mu\text{-}SC_3H_6S)Ni_2(dppe)_2]$- $(BF_4)_2$. Single crystals of $[(\mu\text{-}SC_3H_6S)Ni_2(dppe)_2](BF_4)_2$, **8**, were obtained by slow ether diffusion into an acetonitrile solution, and an X-ray diffraction study was carried out. The structure confirms that the dication contains two square planar nickel centers symmetrically bridged by an η^2- propanedithiolate ligand. A perspective drawing of the dication is shown in Figure 2, and selected bond distances and angles are included in Table 2. The two dithiolate sulfurs lie above the plane of the Ni−Ni vector. The Ni−S distances are all very similar at 2.22 Å and the Ni−S−Ni angles, which are identical within error, average 80.5°. The dihedral angle between each nickel square plane is 128.45 (9)°, and the Ni−Ni distance is 2.871(1) Å.

In the previously reported neutral bis(sulfido) bridged dimer $[(dippe)Ni(\mu\text{-}S)]_2$[12b], the dihedral angle between the nickel square planes increases to 140.2° and the Ni−Ni distance is 2.941(2) Å. Rationales for the nonplanar nature of the $M_2(\mu\text{-}S)_2$ core have been discussed.[12b,17]

(16) Lyon, E. J.; Georgakaki, I. O.; Reibenspies, J. H.; Darensbourg, M. Y. *J. Am. Chem. Soc.* **2001**, *123*, 3268−3278.
(17) Capdevila, M.; Clegg, W.; González-Duarte, P.; Jarid, A.; Lledós, A. *Inorg. Chem.* **1996**, *35*, 490.

Table 3. Electrochemical Data for Nickel Diphosphine/Dithiolate Complexes

Mononuclear Complexes		
complex	$E_{1/2}{}^a$ (ΔE_p, mV)^b PNP^{Et}, Ni(II/I)	$E_{1/2}{}^a$ (ΔE_p, mV)^b PNP^{Ph}, Ni(II/I)
$[Ni(PNP)(S_2CNEt_2)]BF_4$	−1.64 (113)	−1.43^b (110)
$Ni(PNP)(SC_2H_4S)$	−2.34 (110)	−2.02 (74)
$Ni(PNP)(SC_3H_6S)$	−2.26 (131)	−1.94 (77)
$Ni(PNP)(SCH_2C_6H_4CH_2S)$	−2.02 (93)	−1.75 (96)
$[Ni(PNP)(MeSC_2H_4S)]OTf$	−1.47^c (81)	

Dinuclear Complexes		
dithiolate bridge variation	$E_{1/2}{}^a$ (ΔE_p, mV)^b Ni(II/I)	$E_{1/2}{}^a$ (ΔE_p, mV)^b Ni(I/0)
$[Ni(dppe)]_2(SC_2H_4S)^{2+}$, **7**	−1.02 (100)	−2.10 (90)
	−1.18 (100)	−2.47 (105)
$[Ni(dppe)]_2(SC_3H_6S)^{2+}$, **8**	−1.12 (90)	−2.02 (75)
	−1.26 (80)	−2.16 (70)
$[Ni(dppe)]_2(S\text{-}o\text{-xylyl-}S)^{2+}$, **9**	−1.08 (irr)	−2.04 (80)
	−1.30 (irr)	−2.44 (irr)

Diphosphine Variation		
$[Ni(dppe)]_2(SC_3H_6S)^{2+}$, **8**	−1.12 (90)	−2.02 (75)
	−1.26 (80)	−2.16 (70)
$[Ni(dppp)]_2(SC_3H_6S)^{2+}$, **10**	−1.17 (95)	−1.92 (115)
	−1.29 (140)	−2.35 (irr)
		−2.54 (irr)
$[Ni(dppx)]_2(SC_3H_6S)^{2+}$, **12**	−1.13 (140)	−1.75 (160)
	−1.51 (irr)	−1.99 (irr)
		−2.14 (irr)

^{a} $E_{1/2} = (E_{pc} + E_{pa})/2$ reported vs the ferrocene/ferrocenium couple. All experiments were performed at a glassy carbon electrode in 0.3 M Bu_4NBF_4/ CH_3CN at scan rates of 100 or 200 mV/s. Values of $i_{pc}/i_{pa} \cong 1$ unless otherwise noted. ^{b} Each value of ΔE_p is similar to that of the ferrocene/ ferrocenium couple in the same solution. ^{c} $i_{pc}/i_{pa} \approx 3$.
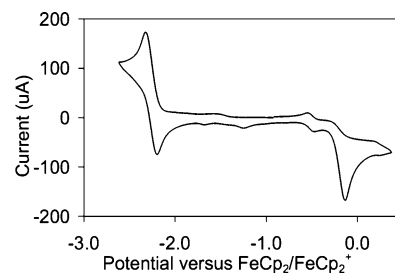
Figure 3. Cyclic voltammogram of $Ni(PNP^{Et})(SC_3H_6S)$ (3×10^{-3} M) recorded at 200 mV/s in CH_3CN/Bu_4NBF_4. Initial scan is negative, starting at −0.8 V. (The sample contains a small amount of decamethylferrocene which shows a reversible wave at −0.51 V.)

Electrochemical Studies. a. Mononuclear Complexes. The electrochemical data for the new nickel complexes are summarized in Table 3. In the series of mononuclear complexes, each of the dithiolate and dithiocarbamate derivatives displays a reversible reduction wave and an irreversible oxidation, as shown in the cyclic voltammogram (CV) for $Ni(PNP^{Et})(SC_3H_6S)$ in Figure 3. (Additional poorly defined waves are observed at more negative potentials.) A coulometric experiment on $Ni(PNP^{Et/SC_2}H_4S)$ carried out at a potential negative of the first reduction wave (−2.7 V) resulted in the passage of 1.05 F per mole of complex, confirming that the wave corresponds to a one-electron process, and this is assigned to the Ni(II/I) couple. In this work we have focused our attention on the half-wave potentials assigned to the Ni(II/I) couples because these are the potentials that have been shown previously to be most

affected by chelate bite size in the [Ni(diphosphine)$_2$]$^{2+}$ complexes. For the series of neutral PNP^{Et}/dithiolate derivatives the $E_{1/2}$ values for the (II/I) couples are all more negative than −2.0 V vs Fc$^{0/+}$. As expected, the anionic thiolate donors make these values much more negative than the Ni-(II/I) half-wave potential for the hydrogen-activating complex, [Ni(PNP^{Et})$_2$]$^{2+}$, observed at −0.64 V vs Fc.

Comparison of the data for the PNP^{Ph} derivatives shows the effect of the phosphine substituents on the half-wave potentials. Each of the waves assigned to the Ni(II/I) couples is ca. 0.3 V more positive than that of the analogous PNP^{Et} complexes. As indicated in Table 3, the cationic dithiocarbamate and thiolate/thioether complexes are significantly easier to reduce than the neutral derivatives. For example, the $E_{1/2}$ value for the first reduction wave for [Ni(PNP^{Et})-(MeSC$_2$H$_4$S)]OTf was found to be −1.47 V vs Fc$^{+/0}$, more than 0.5 V positive of the corresponding dithiolate complex.

In both series of mononuclear dithiolate complexes, the $E_{1/2}$ values shift to more positive values by ca. 80 mV as the size of the dithiolate chelate ring increases from five- to six-membered rings and by ca. 200 mV in going from six- to seven-membered rings. For the bis(diphosphine) complexes, a similar effect of increasing the chelate bite angle on the Ni(II/I) couple was observed for the systematic variation of a single chelate ring.[2,5] The effect was attributed, through both theoretical and structural studies, to a tetrahedral distortion of these complexes that results from an increasingly large dihedral angle between the two planes defined by the two phosphorus atoms of each diphosphine ligand and the metal. This distortion reduces the antibonding overlap between the σ orbitals of the phosphine ligands and the d$_{x^2-y^2}$ orbital of the metal for the LUMO of the complexes. As a result, the energy of the LUMO drops rapidly in energy as the natural bite angle of the ligand increases and the reduction potential becomes less cathodic. Similar effects appear to be in play for these mononuclear dithiolate complexes. The trend in half-wave potentials for these derivatives is consistent with the greater accessibility of a tetrahedrally distorted geometry for the reduced Ni product as the chelate ring size increases. Similar structural distortions imposed by the protein matrix in nickel-containing enzymes may also significantly affect the potentials of the Ni(II/I) couples and provide a mechanism in addition to charge and substituent effects for controlling ease of reduction.

b. Dinuclear Complexes. Within the series of dinuclear complexes, the CVs of all the complexes show similar features. For example, the CV for **8** at a scan rate of 1.0 V/s shows a pair of closely spaced reversible waves at −1.12 and −1.27 V vs Fc$^{+/0}$ that are attributed to the Ni(II/I) couples of electronically coupled metal ions, Figure 4. The waves show slightly less reversible character at a scan rate of 100 or 200 mV/s. Additional reductions near −2 V were also observed, and when the scan direction is reversed at −2.6 V, new anodic waves are observed with E_p at −0.68 and −0.86 V (see Figure S1 for CVs over an expanded range of potentials). The peak potentials for the new anodic waves are very similar to the potentials reported for the oxidation of Ni(dppe)$_2$,[1] suggesting that this monomer is formed in
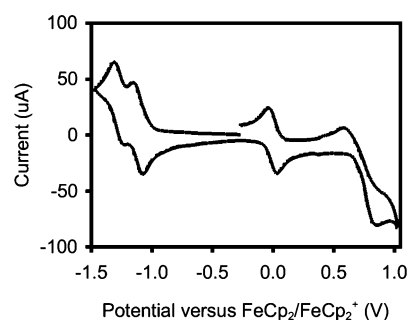
Figure 4. Cyclic voltammogram of **8** (3×10^{-3} M) recorded at a glassy carbon electrode at a scan rate of 1000 mV/s in CH$_3$CN/Et$_4$NBF$_4$. Initial scan direction is negative. The wave at 0.0 V corresponds to the ferrocene/ferrocenium couple used as an internal standard.

the rapid decomposition of the reduced dimer. Further evidence for this decomposition is discussed below. Half-wave potentials for the other dinuclear complexes at scan rates of 100 mV/s are included in Table 3.

In the dinuclear complexes studied here, no systematic trend has been observed for the Ni(II/I) couples as the size of the dithiolate chelate is increased or as the chelate bite angle of the diphosphine ligand is varied (Dinuclear Complexes, Table 3). One possibility for the failure to observe a positive shift in the Ni(II/I) half-wave potential as the number of atoms bridging the dithiolate ligand increases is that the presence of the four-membered Ni$_2$S$_2$ ring controls the S−Ni−S bond angles and minimizes steric interactions between the bridging dithiolate ligand and the two diphosphine ligands. As a result, changing the number of bridging atoms in the dithiolate ligand has little effect on the geometry of the dimer and on the (II/I) or (I/0) couples. A similar insensitivity (as determined by CO stretching frequencies) to the nature of the bridging dithiolate ligands has been reported previously for [(CO)$_3$Fe]$_2$(μ-dithiolate) complexes.[16] The Ni(II/I) couples of the dinuclear complexes are also not affected in a systematic way by an increase in the natural bite angle of the diphosphine ligands. This is tentatively attributed to a minimal steric interaction of the substituents on the diphosphine ligand with the dithiolate bridge.

Reactions of Nickel Complexes with Hydrogen. We wished to determine if the correlation between the Ni(II/I) couple and the hydride acceptor ability observed for [Ni-(diphosphine)$_2$]$^{2+}$ complexes extends to planar Ni(II) complexes with one diphosphine and one dithiolate chelate. To probe the ability of the (PNP)nickel(dithiolate) complexes to activate hydrogen by heterolytic cleavage, they were treated with hydrogen (0.82 atm) in the presence of tetramethylguanadine at room temperature. No reactions were observed for the series of Ni(PNP^{Et})(dithiolate) or Ni(PNP^{Ph})-(dithiolate) complexes, which show Ni(II/I) half-wave potentials over the range of −1.75 to −2.34 V. The dithiocarbamate complex, [Ni(PNP^{Ph})(S$_2$CNEt$_2$)]BF$_4$ ($E_{1/2}$ = −1.43 V vs Fc), reacted in acetonitrile with H$_2$ (0.82 atm) in the presence of tetramethylguanidine over a period of several days (eq 5). No reaction was observed with this base in the absence of hydrogen or with hydrogen and the weaker base, triethylamine. Although the NMR spectrum of the reaction solution showed only resonances for the starting complex

(slightly broadened), over a period of about a week a mixture of yellow and red crystalline precipitates was observed. The reaction was found to involve metal ion reduction, as well as ligand exchange, and the yellow crystals were identified by an X-ray diffraction study as Ni(PNP^{Ph})$_2$, **13**. Structural data on **13** are included in the Supporting Information. The formation of a Ni(0) product may involve metal hydride formation followed by deprotonation, but no hydride intermediate was detected by NMR spectroscopy.

$$[(Et_2NCS_2)Ni(PNP^{Ph})]^+ + H_2 + TMG \rightarrow Ni^0(PNP^{Ph})_2 +$$
$$\text{other products} \quad (5)$$
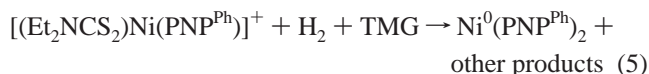
The thiolate/thioether derivative [Ni(PNP)(MeSC$_2$H$_4$S)]BF$_4$ ($E_{1/2}$ = −1.45 V vs Fc) also reacted with hydrogen in the presence of tetramethylguanidine. However, a complex mixture of products was observed in the ^{31}P NMR spectra, and this reaction was not pursued.

Reactions of the Dinuclear Nickel Complexes. The complexes of the formulas [diphosphine)Ni]$_2$(μ-dithiolate)]$^{2+}$ have modest half-wave potentials and we were interested in determining whether this feature permitted reactivity with hydrogen. However, the complexes were not stable in the presence of the strong base tetramethylguanadine, and no reactions with hydrogen (0.8 atm) were observed in the presence of triethylamine. Other aspects of the reduction chemistry of these dimers have also been investigated. The reaction of **8** with 2−4 equiv of PPNBH$_4$ (PPN = bis-(triphenylphosphine)iminium), LiAlH$_4$, or sodium amalgam in THF was monitored by ^{31}P NMR spectroscopy. The reaction proceeded rapidly to completion, and the formation of a single new product was observed by ^{31}P NMR spectroscopy with a resonance at 44.2 ppm. No evidence for formation of a nickel hydride was observed in the corresponding ^{1}H NMR spectrum. The product was identified as the known complex Ni(dppe)$_2$[1] by comparison with an independently prepared sample of the monomer and by further protonation of the reduced product to form the previously reported hydride complex [HNi(dppe)$_2$]$^+$.[2] Ni-(dppe)$_2$ was also the major product observed in the reduction reaction of [(dppeNi)$_2$(μ-SC$_2$H$_4$S)](PF$_6$)$_2$, **7**, with sodium amalgam, although ^{31}P NMR resonances for other unidentified products were also present in this case. These results indicate that the dimeric complexes undergo a decomposition reaction under these reducing conditions, e.g., eq 6. Although
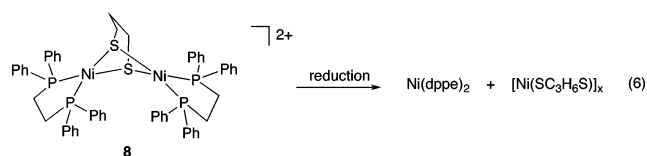
nickel thiolate complexes were not identified in eqs 5 or 6, polynuclear homoleptic nickel(II) complexes with ethane- and propanedithiolate ligands have been characterized previously.[18] The reaction of **8** with tetrabutylammonium cyanide in acetonitrile also resulted in disruption of the dinuclear

structure, and mixtures of mononuclear products, including dppeNi(SC$_3$H$_6$S), dppeNi(CN)$_2$,[19] and (dppe)$_2$Ni, were observed by ^{31}P NMR spectroscopy.

Comparison of Redox Properties for Several Nickel Dimers. A number of unsymmetrical nickel dimers with bridging thiolate ligands have been reported recently as models for a portion of the A-cluster active site in bifunctional CO dehydrogenase/acetyl CoA synthase enzymes.[8] These dimers involve a tetradentate N$_2$S$_2$ nickel complex in which the terminal thiolate ligands bridge to a second nickel-(II) or Ni(0) center.[20−25] In several cases, the second nickel-(II) has been stabilized with the bidentate ligand bis-(diphenylphosphino)ethane, dppe, e.g., structures **14**−**17**.[20−23]
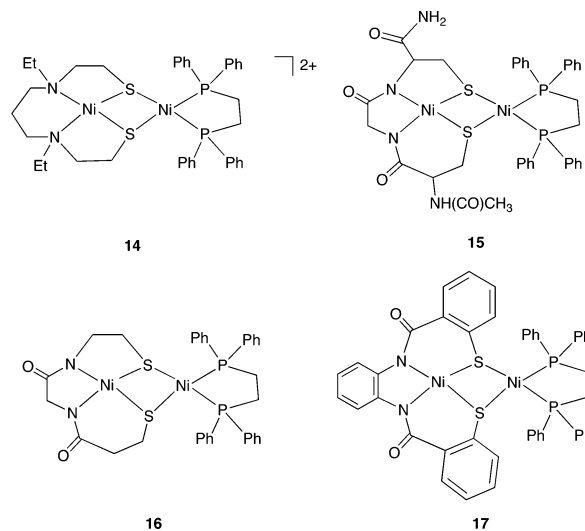
Electrochemical studies of **14** and **15** have revealed a reversible one-electron reduction process attributed to the nickel(dppe) portion of the dimer with additional reductions at more cathodic potentials.[20−21] For the dicationic unsymmetrical dimer **14**, $E_{1/2}$ was reported to be −0.47 V vs SCE in CH$_2$Cl$_2$, or ∼ −0.9 vs ferrocene.[26] Although differences in solvent and reference electrode make comparisons with previous work approximate, the Ni(II/I) half-wave potential is clearly less negative than those observed for the dicationic series of symmetrical dimers reported here (−1.2 vs Fc). A similar trend is observed when the half-wave potential of the *neutral* unsymmetrical dimer **15** is compared with the symmetrical dimers. With similar ligand environments, a neutral complex should be significantly more difficult to

(18) Tremel, W.; Kriege, M.; Krebs, B.; Henkel, G. *Inorg. Chem.* **1988**, *27*, 3886.

(19) Rigo, P.; Corain, B.; Turco, A. *Inorg. Chem.* **1968**, *7*, 1623.

(20) Wang, Q.; Blake, A. J.; Davies, E. S.; McInnes, E. J. L.; Wilson, C.; Schroder, M. *Chem. Commun.* **2003**, 3012.

(21) Krishnan, R.; Riordan, C. G. *J. Am. Chem. Soc.* **2004**, *126*, 4484.

(22) Rao, P. V.; Bhaduri, S.; Jiang, J.; Holm, R. H. *Inorg. Chem.* **2004**, *43*, 5833.
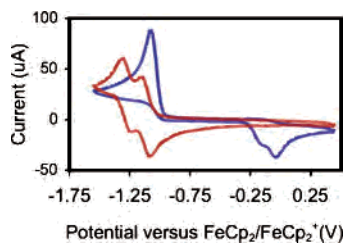
(23) Harrop, T. C.; Olmstead, M. M.; Mascharak, P. K. *J. Am. Chem. Soc.* **2004**, *126*, 14714.

(24) Linck, R. C.; Spahn, C. W.; Rauchfuss, T. B.; Wilson, S. R. *J. Am. Chem. Soc.* **2003**, *125*, 8700.

(25) Golden, M. L.; Rampersad, M. V.; Reibenspies, J. H.; Darensbourg, M. Y. *Chem. Commun.* **2003**, 1824.

(26) In these comparisons, $E_{1/2}$ for the ferrocene/ferrocenium couple is estimated to be +0.40 V vs SCE (Connelly, N. G.; Geiger, W. E. *Chem. Rev.* **1996**, *96*, 879) and +0.54 V vs NHE (Faulkner, L. R.; Bard, A. J. *Electrochemical Methods*; John Wiley and Sons: New York, 2001; p 811).

Figure 5. Cyclic voltammograms for the reduction of **8** under an atmosphere of nitrogen (red scan) and under an atmosphere of carbon monoxide (blue scan) at a scan rate of 1.0 V/s in CH_3CN/Et_4NBF_4.

reduce than a dication (e.g., see Table 3). However, in this case the $E_{1/2}$ for the neutral complex (-0.53 V vs NHE in CH_3CN,[21] or ~ -1.1 vs ferrocene)[26] is in fact similar to the values for the symmetrical dications (-1.2 V vs ferrocene). The potential for **15** occurs at a much less negative value than expected relative to **8**. The overall effect of the N_2S_2Ni "ligand" in **14** and **15** appears to be a withdrawal of electron density from the Ni(dppe) center and a stabilization of the reduced products.

In the study of **15**, the Ni(dppe) center in the presence of CO was proposed to undergo an ECE electrochemical process in which reduction to Ni(I) is followed by CO coordination and further reduction to Ni(0).[20] The one-electron reduction product of **17**, formed from reaction with $NaBH_4$, also reacted with CO to form a (dppe)Ni−CO adduct ($\nu_{CO} = 1997$ cm^{-1}).[23] We wished to determine whether a symmetrical $\{(\mu\text{-dithiolate})[Ni(dppe)]_2\}^{2+}$ showed similar reactivity with carbon monoxide. No reaction of **8** with CO (1 atm) was detected by ^{31}P NMR spectroscopy, but electrochemical studies indicate that the reduced form of **8** does react under these conditions. When the cathodic scan of the CV of the complex is repeated under an atmosphere of CO, a new irreversible reduction wave with increased current intensity occurs with E_p at -1.08 V, and upon reversing the scan direction, irreversible oxidation waves are observed near 0 V, Figure 5. The change in the CV under CO is characteristic of an ECE mechanism involving formation and reduction of a CO adduct.[21] The changes in the CV of **8** are readily reversed when the solution is purged with nitrogen.

Unfortunately, the CO adduct does not appear to be stable on the time scale of a chemical reduction. When the reaction of **8** with $LiAlH_4$ in THF was carried out in the presence of 1 atm of CO over a period of ≤ 1 h, we observed the formation of a new product with a singlet at 46.9 ppm in the ^{31}P NMR spectrum. However, the same product is observed when CO is bubbled into a THF solution of Ni-(dppe)$_2$ and when [Ni(dppe)$_2$]$^{2+}$ is reduced in the presence of CO. The new resonance is therefore assigned to a mononuclear product, tentatively identified as (dppe)Ni(CO)$_2$, which has been previously reported.[27] Thus, under reducing conditions, both the mononuclear complexes and the dinuclear complexes studied in this work tend to form the thermodynamically stable Ni(0) complexes with either CO or phosphine ligands.

Concluding Remarks. Our studies have shown that the half-wave potentials of the Ni(II/I) couples for mononuclear complexes Ni(diphosphine)(dithiolate) shift to more positive values as the chelate ring size of the dithiolate is increased. This presumably occurs through structural distortions similar to those observed previously for [Ni(diphosphine)$_2$]$^{2+}$ complexes. In contrast, the dinuclear nickel complexes with terminal diphosphines and a bridging dithiolate do not show a systematic change in half-wave potentials of the Ni(II/I) couple as the chelate ring size of dithiolate or diphosphine is varied. This does not imply that the tetrahedral distortions imposed by the protein structure on the dinuclear clusters in enzymes do not result in changes in the Ni(II/I) couple. However, attempts to mimic this effect by extending concepts regarding ligand bite angles observed for synthetic mono-nuclear complexes to synthetic dinuclear complexes will likely not be productive.

Experimental Section

Instrumentation. ^1H, ^{13}C, and ^{31}P NMR spectra were recorded on a Varian Inova 400 MHz spectrometer. ^1H and ^{13}C chemical shifts are reported in ppm and are referenced to residual solvent protons. ^{31}P NMR spectra were proton-decoupled, and chemical shifts in ppm are referenced to external phosphoric acid. Hetero-nuclear multiple quantum coherence (HMQC), field gradient heteronuclear single quantum coherence (gHSQC), and $^1H-^1H$ correlation spectroscopy (COSY) NMR experiments were carried out on the Inova instrument in order to assign ^{13}C and ^1H shifts. Electrospray ionization (ESI) mass spectra were collected using an HP 59987A electrospray with an HP 5989B mass spectrometer. Electronic spectra were recorded on an Agilent 8453 UV−vis spectrometer. CVs were obtained at 21 ± 2 °C using a Cypress Systems model CS-1200 computer-aided electrolysis system with a three-electrode arrangement. The working electrode was a glassy carbon disk with a 2 mm diameter, and the counter electrode was a glassy carbon rod with a 3 mm diameter. The pseudo-reference electrode was a silver chloride-coated silver wire. Either ferrocene (Cp$_2$Fe) or decamethylferrocene (Cp*$_2$Fe) ($E_{1/2} = 0.51$ vs [Cp$_2$Fe]$^{0/+}$) was added to the solution as an internal standard after recording the CV of each nickel complex, and all reported potentials are referenced to the [Cp$_2$Fe]$^{0/+}$ couple. CVs were recorded at a scan rate of 100 or 200 mV/s, unless otherwise indicated, under a nitrogen atmosphere in 0.3 M Et$_4$NBF$_4$/acetonitrile solutions. Elemental analyses were performed by Desert Analytics Laboratory, Tucson, AZ.

Methods and Materials. All reactions were carried out using standard Schlenk or glove box techniques under a nitrogen atmosphere. Solvents were dried by conventional methods and distilled prior to use. Dithiol and most diphosphine reagents were purchased from commercial suppliers and used without purification. PNP^{Et},[11] [Ni(CH$_3$CN)$_6$](BF$_4$)$_2$,[28] (dppp)NiCl$_2$,[29] (dppe)NiCl$_2$,[30] (dp-px)NiCl$_2$,[31] (dppe)Ni(SC$_3$H$_6$S),[10k] (dppe)Ni(SC$_2$H$_4$S),[10h] and (dppe)-Ni(SCH$_2$C$_6$H$_4$CH$_2$S)[10g] were synthesized by published procedures.

Controlled-Potential Coulometry. A cell containing two com-partments separated by a Nafion membrane was used for this

---

(27) Sacco, A.; Mastrorilli, P. *J. Chem. Soc., Dalton. Trans*. **1994**, 2761.

(28) Hathaway, B. J.; Holah, D. G.; Underhill, A. E. *J. Chem. Soc*. **1962**, 2444.
(29) Van Hecke, G. R.; Horrocks, W. D. *Inorg. Chem*. **1966**, *5*, 1968.
(30) Booth, G.; Chatt, J. *J. Chem Soc*. **1965**, 3238.
(31) (a) Brown, M. D.; Levason, W.; Reid, G.; Watts, R. *Polyhedron* **2005**, *24*, 75. (b) Camalli, M.; Caruso, F.; Chaloupka, S.; Leber, E. M.; Rimml, H.; Venanzi, L. M. *Helv. Chim. Acta* **1990**, *73*, 2264.

experiment. Reticulated vitreous carbon (1 cm diameter × 2.5 cm length) was used as the working electrode. A glass tube fitted with a Vycor frit at the bottom, containing 0.3 M Bu$_4$NBF$_4$ solution and a silver wire was also inserted into the working half of the cell. In the other half of the cell a platinum wire in a solution of ferrocene/ferrocenium was used as the counter electrode. The working half of the cell was typically filled with 10 mL of 0.3 M Bu$_4$NBF$_4$ in acetonitrile. [Ni(PNP)(SC$_2$H$_4$S)] (0.093 mmol) was added to the solution. Controlled-potential coulometry was performed at −2.70 V versus the ferrocene/ferrocenium reference electrode. A total of 9.48 C of charge was passed before the current decayed to background levels. This corresponds to 1.05 F per mole of catalyst, and it supports a one-electron process for the first reduction wave.

Synthesis of (PNP^{Ph}). A round-bottom flask was charged with diphenylphosphine (10.40 g, 56.4 mmol) and degassed aqueous formaldehyde (37 wt %, 4.40 mL, 58.7 mmol) in ethanol (20 mL). After the solution was stirred for 30 min, CH$_3$NH$_3$Cl (1.80 g, 26.6 mmol) in ethanol /water (8 mL/4 mL) was added. The mixture was stirred at room temperature for 3 h, and the solvent was removed in vacuo. The product was extracted with diethyl ether (3 × 25 mL). Removal of the solvent from the combined extracts produced a viscous oil. Yield: 10.66 g, 24.9 mmol, 94%. The product (10.66 g, 24.9 mmol) was dissolved in CD$_3$CN (3.55 g) to form a standard solution of 75 wt %. ^{1}H NMR (CD$_3$CN): 7.32 and 7.40 (two m, aromatics); 3.43 (d, $^2J_{PH}$ = 4.0 Hz, PCH_2N); 2.58 (s, NCH_3). ^{31}P NMR (CD$_3$CN): −26.66 (s).

Syntheses of Mononuclear Complexes. The syntheses of the mononuclear nickel complexes are all very similar, and the procedures and characterization data are given for only two representative examples. Spectroscopic characterization data for the remaining complexes are given in the Supporting Information.

[Ni(PNP^{Et})(S$_2$CNEt$_2$)](BF$_4$). Solid [Ni(CH$_3$CN)$_{6.5}$](BF$_4$)$_2$ (0.67 g, 1.34 mmol) was added to a solution of PNP^{Et} (0.31 g, 1.33 mmol) and NaS$_2$CNEt$_2$ (0.30 g, 1.34 mmol) in 40 mL of CH$_3$CN. The reaction mixture was stirred overnight at room temperature. The solution was filtered, and the solvent was removed from the filtrate under vacuo. The resulting solid was dissolved in 3 mL of CH$_3$CN and precipitated with 20 mL of Et$_2$O. The dark yellow microcrystalline solid was collected by filtration and washed with 2 × 20 mL of Et$_2$O. Yield: 0.69 g, 1.08 mmol, 81%. Anal. Cacld for C$_{16}$H$_{37}$BF$_4$N$_2$NiP$_2$S$_2$ + 1 NaBF$_4$: C, 30.08; H, 5.84; N, 4.38. Found C, 30.52; H, 5.55; N, 4.31. ^{1}H NMR (CD$_3$CN): 3.73 (q, $^3J_{HH}$ = 7.2 Hz, NCH_2CH$_3$); 2.77 (m, PCH_2N); 2.44 (m, NCH_3); 1.81 (m, PCH_2CH$_3$); 1.27 (dt, $^3J_{PH}$ = 17.4 Hz; $^3J_{HH}$ = 7.9 Hz, PCH$_2$CH_3); 1.26 (tr, $^3J_{HH}$ = 7.2 Hz, NCH$_2$CH_3). ^{13}C NMR (CD$_3$CN): (Assignments are supported by dept and HSQC data.) 200.8 (s, NCS); 50.8 (tr, $^1J_{PC}$ = 21.8 Hz, PCH$_2$N); 50.1 (tr, $^3J_{PC}$ = 12.5 Hz, NCH$_3$); 44.7 (s, NCH$_2$CH$_3$); 17.6 (tr, $^1J_{PC}$ = 14.2 Hz, PCH$_2$CH$_3$); 11.9 (s, NCH$_2$$CH_3$); 8.5 (s, PCH$_2$$CH_3$). ^{31}P NMR (CD$_3$CN): 15.5 (s). MS [Ni(PNP)(S$_2$CNEt$_2$)]$^+$ − H$_2$ simulated max m/z 439; found max m/z 439 with matching isotope pattern. CV (CH$_3$CN): $E_{1/2}$, V vs ferrocene (ΔE_p, mV): −1.64 (113). Oxidation, E_p, 0.08 (irrev).

(PNP^{Ph})Ni(SC$_3$H$_6$S). Solid [Ni(CH$_3$CN)$_{6.5}$](BF$_4$)$_2$ (0.50 g, 1.0 mmol) was added to a solution of PNP^{Ph} (0.43 g, 1.00 mmol) and HSC$_3$H$_6$SH (0.11 g, 1.0 mmol) in 30 mL of CH$_3$CN, upon which a deep red color was observed. After the solution was stirred for 20 min, NEt$_3$ (0.25 g, 2.47 mmol) was added. The solution, which turned a darker red, was stirred for 2 h. The solvent was removed under vacuo until ∼2 mL of solution remained, and the resulting precipitate was filtered and dried under vacuum. The product was recrystallized from ∼2 mL of CH$_3$CN. Resulting red crystals were filtered, washed with 3 × 25 mL hexanes, and dried overnight under

vacuum. Yield: 0.12 g, 0.20 mmol, 20%. ^{1}H NMR (CD$_3$CN): 7.79 (m, *meta*-aromatics); 7.44 (apparent tr, *para*-aromatics); 7.37 (apparent tr, *ortho*-aromatics); 3.22 (apparent tr, PCH_2N); 2.32 (m, NCH_3); 2.19 (m, SCH_2). ^{31}P NMR (CD$_3$CN): 9.53 (s). Anal. Calcd for C$_{30}$H$_{33}$NNiP$_2$S$_2$: C, 60.83; H, 5.62; N, 2.36. Found: C, 60.59; H, 5.86; N, 2.20. CV (CH$_3$CN): $E_{1/2}$, V vs ferrocene (ΔE_p, mV): −1.94 (77). Oxidation, E_p, −0.11 (irrev).

Syntheses of Dinuclear Complexes. The syntheses of the dinuclear nickel complexes follow two routes, and the procedures and characterization data are given for two representative examples. The characterization data for the remaining complexes are given in the Supporting Information.

Synthesis of [(μ-SC$_3$H$_6$S)Ni$_2$(dppe)$_2$](BF$_4$)$_2$. Solid 1,2-bis-(diphenylphosphino)ethane (0.092 g, 0.23 mmol) was added to a solution of [Ni(CH$_3$CN)$_{6.5}$](BF$_4$) (0.115 g, 0.230 mmol) in acetonitrile (10 mL). Solid Ni(dppe)(SC$_3$H$_6$S) (0.13 g, 0.23 mmol) was then added to the resulting yellow solution. The dark red solution was stirred at room temperature for 3 h and then dried in vacuum. An acetonitrile solution of the resulting red oil yielded red crystals by ether diffusion. Yield: 0.214 g, 78%. Anal. Calcd for C$_{55}$H$_{54}$P$_4$S$_2$B$_2$F$_8$Ni$_2$: C, 55.32; H, 4.56. Found: C, 55.12; H, 4.38. ^{1}H and ^{13}C resonances are assigned on the basis of gCOSY, gHSQC, and gHMQC experiments. ^{1}H NMR (20 °C, CDCl$_3$): 7.62−7.42 (40H, m, PC$_6$H$_5$); 2.76 (8H, broad m, PCH_2CH_2); 2.23 (2H, broad s, SCH$_2$CH_2CH$_2$); 2.14 (4H, broad s, SCH_2CH$_2$CH_2). ^{31}P NMR (CDCl$_3$): 60.01 (s). ^{13}C NMR (CDCl$_3$): 133.5−126.7 ppm (PC_6H$_5$); 36.0 (s, SCH$_2$$CH_2CH_2$); 32.3 (s, SC$H_2CH_2$$CH_2$); 27.7 (m, P$CH_2CH_2$). ESI$^+$ (CH$_3$OH): m/z 1107 {[(μ-SC$_3$H$_6$S)Ni$_2$(dppe)$_2$](BF$_4$)}$^+$; m/z 509 [(μ-SC$_3$H$_6$S)Ni$_2$(dppe)$_2$]$^{2+}$. CV at 1000 mV/s (CH$_3$CN): $E_{1/2}$ or E_p if irreversible, V vs ferrocene (ΔE_p, mV): −1.12 (74); −1.27 (80); −2.20 (80); −2.51 (irrev); −2.66 (irrev). Oxidations: 0.73 (270). UV−vis, (CH$_3$CN) λ_{max}, nm (ϵ, M^{-1} cm^{-1}): 281 (46 900); 351 (23 400).

[(μ-SC$_3$H$_6$S)Ni$_2$(dppx)$_2$](PF$_6$)$_2$ Solutions of 1,3-propanedithiol (12 μL, 0.12 mmol) in chloroform (5 mL) and triethylamine (0.26 mL, 1.8 mmol) in chloroform (5 mL) were added to a solution of Ni(dppx)Cl$_2$ (0.150 g, 0.248 mmol) in chloroform (15 mL). The resulting brown solution was stirred at room temperature for 1 h, and the volume was reduced to 10 mL. A solution of NaPF$_6$ (0.13 g, 0.25 mmol) in 1:1 ethanol/water (15 mL) was added, and the resulting orange precipitate was filtered. Yield: 0.073 g, 40%. Anal. Calcd for C$_{67}$H$_{62}$P$_6$S$_2$F$_{12}$Ni$_2$: C, 55.02; H, 4.27. Found: C, 54.84; H, 4.48. ^{1}H and ^{13}C resonances are assigned on the basis of gHMQC experiments. ^{1}H NMR (CD$_3$CN): 7.93−7.46 (40H, m, PC$_6$H$_5$); 6.64 (4H, m, PCH$_2$CCH); 6.08 (4H, m, PCH$_2$CCHCH); 4.53 (4H, pseudo d, PCH_2); 3.45 (4H, broad m, PCH_2); 1.71 (2H, broad m, SCH$_2$CH_2-CH$_2$); 0.04 (4H, broad m, SCH_2CH$_2$CH_2). ^{31}P NMR (CD$_3$CN): 11.01 (s). ^{13}C NMR (CD$_3$CN): 136.3−127.2 (PC_6H$_5$); 131.7 (s, PCH$_2$CCHCH); 128.3 (s, PCH$_2$CCH); 37.4 (s, SCH$_2$CH$_2$$CH_2$); 35.4 (s, SCH$_2$$CH_2CH_2$); 34.22 (s, P$CH_2C_6H_4$$CH_2$). ESI$^+$ (CH$_3$CN): m/z 1318 {[(μ-SC$_3$H$_6$S)Ni$_2$(dppx)$_2$](PF$_6$)}$^+$; m/z 584 [(μ-SC$_3$H$_6$S)Ni$_2$-(dppx)$_2$]$^{2+}$. CV (CH$_3$CN): $E_{1/2}$ or E_p if irreversible, V vs ferrocene (ΔE_p, mV): −1.13 (140); −1.51 (irrev); −1.75 (160); −1.99 (irrev); −2.14 (irrev). Oxidations: 0.75 (irrev); 0.92 (irrev); 1.4 (irrev). UV−vis (CH$_3$CN), λ_{max}, nm (ϵ, M^{-1} cm^{-1}): 304 (67 000); 395 (40 000).

Reduction of [(μ-SC$_3$H$_6$S)Ni$_2$(dppe)$_2$](BF$_4$)$_2$, 5. In a typical procedure monitored by NMR spectroscopy, solid LiAlH$_4$ (0.002 g, 0.05 mmol) was added to a solution of **5** (0.020 g, 0.017 mmol) in THF in an NMR tube. The resulting dark greenish brown solution was shaken for 10 min. A single product was observed by ^{31}P NMR-(THF): 44.2 ppm (Ni(dppe)$_2$). On a larger scale, a flask was charged with solid [(μ-SC$_3$H$_6$S)Ni$_2$(dppe)$_2$](BF$_4$)$_2$ (0.050 g, 0.042 mmol)

Table 4. Details of Data Collection and Structure Refinement for [Ni(PNP^{Et})(SC$_2$H$_4$SMe)]OTf, **6**, and [(μ-SC$_3$H$_6$S)Ni$_2$(dppe)$_2$](BF$_4$)$_2$·CH$_3$CN, **8**

	C$_{57}$H$_{57}$B$_2$F$_8$NNi$_2$P$_4$S$_2$, **8**	C$_{15}$H$_{34}$F$_3$NNiO$_3$P$_2$S$_3$, **6**
empirical formula	C$_{57}$H$_{57}$B$_2$F$_8$NNi$_2$P$_4$S$_2$, **8**	C$_{15}$H$_{34}$F$_3$NNiO$_3$P$_2$S$_3$, **6**
fw	1235.06	550.26
T, K	143(2)	143(2)
cryst syst	monoclinic	triclinic
space group	$P2_1/c$	$P\bar{1}$
a (Å)	12.1836(5)	8.781(3)
b (Å)	47.750(2)	10.217(3)
c (Å)	10.3067(4)	14.543(4)
α (deg)	90	71.276(7)
β (deg)	107.914 (1)	82.684(7)
γ (deg)	90	81.593(7)
V (Å^3)	5705.4(4)	1218.0(6)
Z	4	2
density (calcd) (mg m^{-3})	1.435	1.500
abs coeff (mm^{-1})	0.910	1.224
reflns measd/indep	45 702/13 090	9693/5580
GOF	0.951	1.045
R1 [$I > 2\sigma(I)$] (all data)	0.0808 (0.1783)	0.0978 (0.1526)
wR2 [$I > 2\sigma(I)$] (all data)	0.1621 (0.1885)	0.2568 (0.3083)
largest diff. peak and hole (e/Å^3)	0.679 and −0.605	1.943 and −1.131

and 1% sodium/mercury amalgam (1.87 g Na/Hg, 0.084 mmol Na). Acetonitrile (10 mL) was added, and the reaction mixture was stirred overnight. The cloudy reddish-brown solution was removed from the mercury and then dried in vacuum. ^{31}P NMR (THF): 44.2 ppm (Ni(dppe)$_2$). The sodium/amalgam reduction was also carried out in THF, and the same product was observed. Addition of HBF$_4$·Et$_2$O to the reduced product resulted in the formation of [HNi-(dppe)$_2$]BF$_4$. ^{31}P NMR (THF): 45.48 (CD$_3$CN): 45.72. ^{1}H NMR (CD$_3$CN): 7.34−7.20 (40H, m, PC$_6$H$_5$); 2.39 (8H, m, PCH$_2$CH$_2$P); −12.99 (1H, pent, NiH).

X-ray Diffraction Studies. For each structure, a crystal of appropriate size was mounted on a glass fiber using Paratone-N oil, transferred to a Siemens SMART diffractometer/CCD area detector, centered in the beam (Mo Kα; $\lambda = 0.71073$ Å; graphite monochromator), and cooled to −120 ± 10 °C by a nitrogen low-temperature apparatus. Preliminary orientation matrix and cell constants were determined by collection of 60 frames, followed by spot integration and least-squares refinement. A minimum of a hemisphere of data was collected using 0.3° ω scans. The raw data were integrated and the unit cell parameters refined using SAINT. Data analysis was performed using XPREP. Absorption correction was applied using SADABS. The data were corrected for Lorentz and polarization effects, but no correction for crystal decay was applied. Structure solutions and refinements were performed (SHELXTL-Plus V5.0) on F^2.[32] All non-hydrogen atoms were refined anisotropically. Hydrogens were placed in idealized posi-

tions and were included in structure factor calculations but were not refined. Details of the data collection, structure solution, and refinement are given in Table 4.

Supporting Information Available: Characterization data for additional complexes, Figure S1 and X-ray structural data including tables of crystal and refinement data, atomic positional and thermal parameters and interatomic distances and angles for **5**, **8**, and **13**. This material is available free of charge via the Internet at http://pubs.acs.org.

IC061740X

(32) Sheldrick, G. M. *SHELXTL-Plus: A Program for Crystal Structure Determination*, version 5.1; Bruker AXS: Madison, WI, 1998.